Large enhancement of interface second-harmonic generation near the zero-$\bar{n}$ gap of a negative-index Bragg grating

Giuseppe D'Aguanno,[1,2,*] Nadia Mattiucci,[2,3] Mark J. Bloemer,[1] and Michael Scalora[1]
[1]*Charles M. Bowden Research Center, RDECOM Building 7804, Redstone Arsenal, Alabama 35898-5000, USA*
[2]*Time Domain Corporation, Cummings Research Park, 7057 Old Madison Pike, Huntsville, Alabama 35806, USA*
[3]*Dipartimento di Fisica "E. Amaldi," Università "RomaTre," Via Della Vasca Navale 84, I-00146 Rome, Italy*
(Received 19 August 2005; revised manuscript received 29 December 2005; published 6 March 2006)

We predict a large enhancement of interface second-harmonic generation near the zero-$\bar{n}$ gap of a Bragg grating made of alternating layers of negative- and positive-index materials. Field localization and coherent oscillations of the nonlinear dipoles located at the structure's interfaces conspire to yield conversion efficiencies at least an order of magnitude greater than those achievable in the same length of nonlinear, phase-matched bulk material. These findings thus point to a new class of second-harmonic-generation devices made of standard centrosymmetric materials.

DOI: 10.1103/PhysRevE.73.036603 PACS number(s): 42.70.Qs, 42.65.Ky, 42.79.Dj, 78.20.Ci

In nonlinear optics, it is well known that in the dipole approximation, only materials that lack inversion symmetry, e.g., the III-V semiconductors, exhibit a nonvanishing bulk quadratic coefficient [1]. In practice, this fact limits the range of materials that may be used for optical processes that involve quadratic interactions, such as second-harmonic generation (SHG) and parametric frequency up- and down-conversion. Although materials with inversion symmetry do not possess bulk quadratic nonlinearity, they do nevertheless exhibit surface quadratic nonlinearity. These nonlinearities originate with the lack of inversion symmetry that occurs within a few atomic or molecular layers near the surface of the material, due to both structural and field discontinuities [2].

One might think it is possible to take advantage of surface nonlinearities of this kind by using a multilayer N-period Bragg grating, and by exploiting the conditions that maximize coherent emission from the centers of nonlinearity, in this case located at each interface within the structure. The fundamental frequency (FF) field should then be tuned at a band edge, where a high density of modes is accompanied by high field localization. In fact, it has already been demonstrated both theoretically [3] and experimentally [4] that near the band edge a combination of high field localization and phase-matching conditions can enhance second- [4(a)] and third-order [4(b)] nonlinear optical processes. Unfortunately, in conventional N-period Bragg gratings, or finite photonic band gap (PBG) structures, field localization properties at the band edges are such that the field is localized in either the high- or the low-index layers, but never at any of the interfaces, where instead the field achieves local minima. Moreover, adding more periods to the structure further reduces the magnitude of the local minima, and field values quickly approach zero. Therefore, the inescapable consequence is that conventional Bragg gratings made with positive-index, centrosymmetric materials (PIMs) are ill suited for nonlinear frequency conversion due to field localization properties that may instead lead to inhibition of surface emissions.

Within the last few years, another class of artificial materials has captured the attention of the scientific community. Known as left-handed or negative-index materials (NIMs), these materials simultaneously display negative electric susceptibility and magnetic permeability [5–7]. The most impressive property of NIMs may well be their ability to refract the light in the opposite way with respect to what an ordinary material does [8] due to a negative refractive index, and several applications have been proposed. For example, we cite the possibility to construct a "perfect" lens, i.e., a lens that can also focus evanescent, near-field waves emanating from a source located near a NIM [5]. Another intriguing property is that a one-dimensional structure made of alternating layers of negative- and positive-index materials (NIM/PIM), such that the index of refraction averages to zero inside the elementary cell, opens a Bragg gap centered about the frequency where the condition $\bar{n}=0$ is satisfied [9]. This so-called zero-$\bar{n}$ Bragg gap is unique because it cannot be replicated, and its properties are different compared to conventional Bragg gratings made of PIMs. For example, strong beam modification and reshaping of tunneling pulses have been predicted [10] while the location and depth of the gap are relatively insensitive to disorder [9] and to the incident angle [11]. In the nonlinear regime, it has also been shown that this zero-$\bar{n}$ Bragg gap can support omnidirectional gap solitons in the presence of a Kerr nonlinearity [12].

In this paper we study surface SHG from a NIM/PIM Bragg grating, and show that tuning the FF at the high-frequency band edge of the zero-$\bar{n}$ gap leads to at least an order of magnitude enhancement of conversion efficiency compared to generation from a PIM having similar length and nonlinear coefficient. This surprising outcome appears to be directly related to the peculiar field localization properties at the high-frequency band edge of the zero-$\bar{n}$ Bragg gap, which have no counterpart in a PIM Bragg grating. In Fig. 1 we show the transmission of an ($N=35$)-period NIM/PIM Bragg grating. The electric susceptibility and the magnetic permeability of the NIM are described by a lossy Drude model [13]: $\varepsilon(\tilde{\omega})=1-1/[\tilde{\omega}(\tilde{\omega}$

*Email address: giuseppe.daguanno@gmail.com

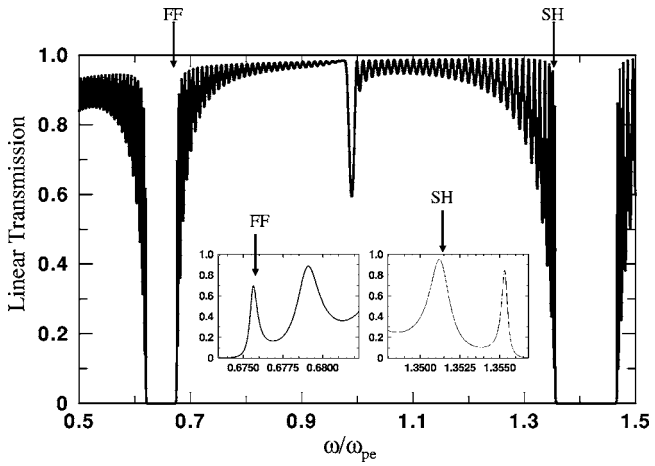

FIG. 1. Transmission vs normalized frequency ω/ω_{pe} for $N=35$ periods of alternating NIM/PIM layers. The thicknesses of the layers are $a=b=0.36\lambda_{pe}$, and $\lambda_{pe}=2\pi c/\omega_{pe}$. The PIM is assumed to be a normal dispersive material having linear dispersion between the FF and the SH frequency. Here we have $n_{\mathrm{FF,PIM}}=1.4$ and $n_{\mathrm{SH,PIM}}\cong 1.466$. The dispersion of the NIM is described by a lossy Drude model, as detailed in the main text. The arrows indicate tuning of the FF and SH. Inset: Magnification of the tuning conditions for the FF and SH.

$+i\tilde{\gamma}_e)]$, $\mu(\tilde{\omega})=1-(\omega_{pm}/\omega_{pe})^2/[\tilde{\omega}(\tilde{\omega}+i\tilde{\gamma}_m)]$, where $\tilde{\omega}=\omega/\omega_{pe}$ is the normalized frequency, ω_{pe} and ω_{pm} are the respective electric and magnetic plasma frequencies, and $\tilde{\gamma}_e=\gamma_e/\omega_{pe}$ and $\tilde{\gamma}_m=\gamma_m/\omega_{pe}$ are the corresponding electric and magnetic loss terms normalized with respect to the electric plasma frequency. For simplicity we assume $\omega_{pm}=\omega_{pe}$ and $\tilde{\gamma}_e\sim\tilde{\gamma}_m\sim 10^{-4}$. The details of the structure are described in the caption of the figure. The PIM is assumed to have normal linear dispersion between the FF and SH frequencies, with $n_{\mathrm{FF,PIM}}=1.4$ and $n_{\mathrm{SH,PIM}}\cong 1.466$. The structure was designed so that the SH would be tuned near the low-frequency band edge of the second normal Bragg gap instead of the first. The reason for this particular kind of tuning can be easily understood if we plot the Bloch vector K_β of the elementary cell of the structure (see Fig. 2). Momentum conservation requires that $\Delta K_\beta=K_\beta(2\omega)-2K_\beta(\omega)\cong G_m$ where $G_m=2\pi m/\Lambda$ is one of the reciprocal lattice vectors, $\Lambda=a+b$ is the length of the elementary cell, and m is an integer number. From Fig. 2 we see that tuning the SH near the first conventional Bragg gap would have resulted in momentum nonconservation: $\Delta K_\beta\cong G_1/2$. Tuning the SH near the second conventional Bragg gap results in momentum quasiconservation, i.e., $\Delta K_\beta\cong 0$. In conventional Bragg gratings momentum conservation is achieved by tuning the FF and SH respectively near the first and the second Bragg gaps so that $\Delta K_\beta\cong G_1$.

In Fig. 3 we plot the FF field profile. The figure shows that the field becomes localized inside the structure under a bell-shaped envelope typical of field envelopes found near band edge resonances of conventional Bragg gratings. However, unlike conventional Bragg gratings, each field maximum coincides exactly with each interface inside the structure. The generated SH field was calculated in the undepleted pump regime according to the following formula:

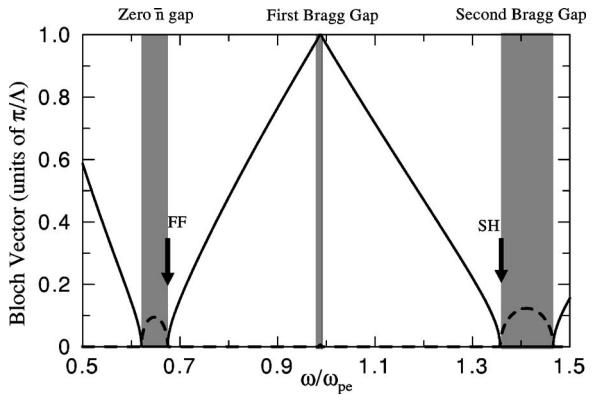

FIG. 2. Real (solid line) and imaginary (dashed line) parts of the Bloch vector vs ω/ω_{pe}. The Bloch vector is calculated for the elementary cell of the structure described in Fig. 1, which has length $\Lambda=a+b$. The arrows indicate tuning of the FF and SH. The shaded regions indicate the spectral positions of the gaps.

$$E_{\mathrm{SH}}(z)=-4\frac{\omega^2}{c^2}\int_0^L G_{\mathrm{SH}}(\xi,z)d^{(2)}(\xi)E_{\mathrm{FF}}^2(\xi)d\xi \qquad (1)$$

where $G_{\mathrm{SH}}(\xi,z)$ is the Green's function of a generic multilayer structure [14], appropriately modified to handle magnetically active materials [15]. $L=N\Lambda$ is the total length of the structure and Λ is the length of the elementary cell. $d^{(2)}(z)$ is the quadratic coupling coefficient, which is assumed to be a sum of Dirac δ functions, each located at the different interfaces of the structure, i.e., $d^{(2)}(z)=d_s^{(2)}\Sigma_j\delta(z-z_j)$, where z_j is the position of the jth interface. For simplicity we have assumed the same value of interface nonlinearity $d_S^{(2)}$ for all the interfaces of the structure, including entrance and exit surfaces. In Fig. 4 we show the generated SH field inside the structure for $d_S^{(2)}|E_{\mathrm{FF,input}}|=10^{-5}$. The SH field is generated with a double bell-shaped envelope, again consistent with its tuning at the second transmission resonance near the second, normal Bragg gap [16], as shown in the inset of Fig. 1.

In Fig. 5 we compare the SH emitted from this structure

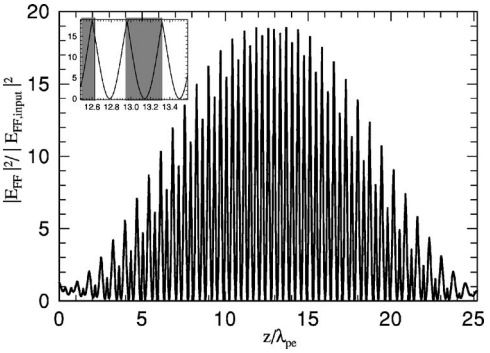

FIG. 3. Localization of the FF field inside the structure. Inset: Magnification of the field near the center of the structure. The field is highly localized at each interface of the structure. The shaded region represents the layer of NIM, while the white region corresponds to layers of PIM.

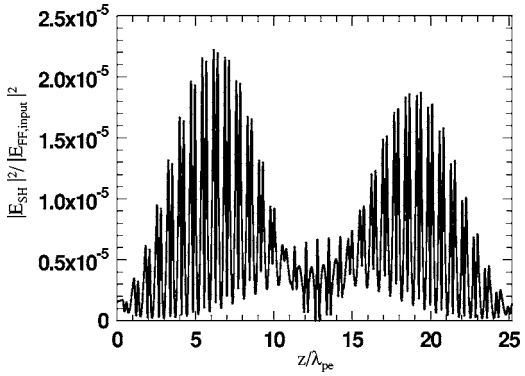

FIG. 4. SH field generated inside the structure for $d_S^{(2)}|E_{\mathrm{FF,input}}|=10^{-5}$.

with the SH emitted from a bulk material in perfect phase matching, having the same nonlinearity $d_S^{(2)}$ and length as our structure. The calculation was performed as a function of SH tuning with respect to its gap on the low-frequency side, in a frequency range that includes the third resonance as well as gap regions. The different tuning conditions were obtained by varying the dispersion of the PIM at the SH. Using this procedure one can find optimal tuning conditions for SHG with respect to the band edge. For example, choosing $n_{\mathrm{SH,PIM}}\cong 1.4538$ tunes the SH field at the third transmission resonance; $n_{\mathrm{SH,PIM}}\cong 1.466$ tunes it at the second transmission resonance, as in Fig. 1; and $n_{\mathrm{SH,PIM}}\cong 1.4739$ tunes it at the first transmission resonance. Tuning the SH at the second transmission resonance results in the highest conversion efficiency, about five times greater than in the same length of phase-matched bulk material. We also find that SH emission is slightly unbalanced in favor of the backward direction.

In order to draw some more general considerations, in Fig. 6 we plot the SH conversion efficiency for one of the conditions corresponding to Fig. 5, i.e., tuning at the second transmission resonance for $N=16$, 18, 25, 30, and 35 period structures, respectively. We find that the conversion efficiency scales roughly as N^6, in analogy with what happens in positive-index PBG structures [16]. Therefore, adding just a

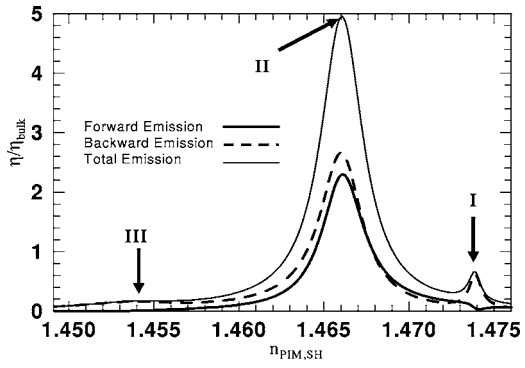

FIG. 5. Normalized SH conversion efficiency η vs $n_{\mathrm{SH,PIM}}$ normalized with respect to the conversion efficiency of a bulk material of the same length and nonlinear coefficient, in perfect phase matching. The arrows correspond, respectively, to the first three transmission resonances near the low-frequency band edge of the second Bragg gap, as labeled.

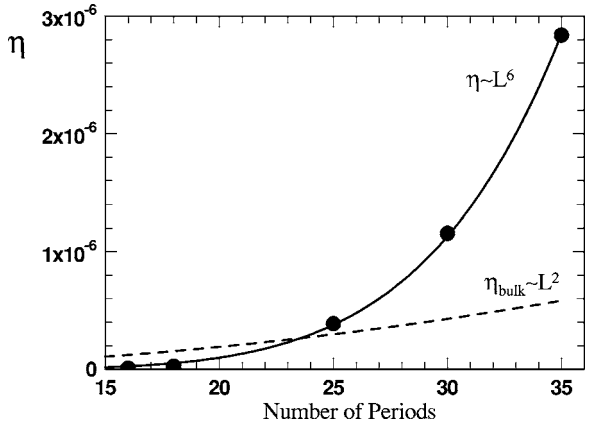

FIG. 6. Total (forward+backward) conversion efficiency vs number of periods for the SH tuned at the second transmission resonance near the low-frequency band edge of the second conventional Bragg gap (solid line and solid circles) and for an ordinary bulk quadratic material in perfect phase matching having the same length and nonlinear coefficient (dashed line). The solid circles correspond to calculated data, the solid line is a fitting curve. We have assumed $d_S^{(2)}|E_{\mathrm{FF,input}}|=10^{-5}$ in all cases. Note that the conversion efficiency of the Bragg grating scales as the sixth power of the length or the number of periods.

few more periods would result in conversion efficiencies more than one order of magnitude greater than those achievable in a generic, quadratic, bulk material in perfect phase matching and with the same quadratic coefficient. Finally, it is evident that recent advancements in the field of metamaterials suggest that NIMs operating in the mid- and near-infrared regime may be within reach [17–22]. In particular, NIMs in the mid- and near-infrared regime have been realized and experimentally tested in Refs. [19–22]. In this context it is also worth mentioning the work by Ishikawa *et al.* [23] where the possibility of negative permeability in composite split-ring resonators is theoretically investigated for optical frequencies. The results presented in Refs. [19–22] put our work on a more solid ground, allowing for more practical tests of our theoretical findings. In the present context, setting our reference wavelength to $\lambda=1$ μm makes our structure approximately 25 μm thick. It is also worth noting that recently one-dimensional structures made of alternating layers of NIM/PIM similar to those described in our paper have been theoretically demonstrated to show a complete three-dimensional band gap [24].

It is worth spending some words on an important issue that stems from our analysis, namely, the effect of the absorption. In our analysis we have used a lossy Drude model in order to describe the dispersion properties of the NIM, a model that has been widely used in published literature [5,13,25–29] because it retains some of the salient characteristics of the physical mechanisms that lead to negative refraction. In our calculations the absorption coefficient for both the electric and magnetic parts has been set to $\tilde{\gamma}_e\sim\tilde{\gamma}_m\sim 10^{-4}$. Of course, increasing the value of the absorption coefficient would result in the lowering of the transmission resonances which ultimately leads to decrease in the SH conversion efficiency. In currently available metamaterials

[19–22] in the mid- and near-infrared regime the issue of the absorption and/or loss may still represent a serious obstacle for several practical applications including the one we are proposing in this paper. On the other hand, while the causality principle requires that the real and imaginary parts of the dispersion of a medium be Kramers-Kronig pairs, it does not put a limit to how small the absorption of a medium should be, as long as it is not zero. The real and imaginary parts of both ε and μ in our lossy Drude model are in fact Kramers-Kronig pairs regardless of how small the electric and magnetic loss terms may be. Therefore, at least in principle, nothing prevents the availability of NIMs with small losses in the near future.

Another issue that may arise from our analysis is the origin of the quadratic nonlinearity at the NIM/PIM interface. A detailed analysis of the quadratic nonlinearity in a NIM material is out of the scope of the present work. In the present context, the main source of nonlinearity must be that stemming from the symmetry breaking near the PIM surface, a PIM that is considered as a standard centrosymmetric material, as we also made clear in the introduction of this work. The considerations about the origin of the quadratic nonlinearity due to symmetry breaking are therefore intended to be valid just for the PIM and by no means are intended for the NIM. A NIM may or may not have a quadratic nonlinearity, but, again, this issue is out of the scope of the present work. We also note that in our calculations, for the sake of simplicity, we have assumed the same value of the quadratic nonlinearity at each interface of our structure including the entrance surface, i.e., the air/NIM interface. Nevertheless, our calculations show that the results remain practically unchanged also if we neglect this first nonlinearity located at the entrance surface.

Finally, it is worth pointing out that although in this work we have considered structures in which the thicknesses of the NIM and PIM layers are the same and therefore also their respective refractive indices at the FF frequency are almost equal in absolute value, nevertheless the same kind of localization as that shown in Fig. 3 is found also in cases in which the thicknesses of the NIM and PIM layers are different, provided that the FF field is tuned near the high-frequency band edge of the zero-$\bar{n}$ gap. Those findings suggest that the kind of field localization just described in this work, i.e., with high field values at the interfaces of the structure, should be a peculiar characteristic of any zero-$\bar{n}$ gap.

In conclusion we have shown that the peculiar localization properties near the zero-$\bar{n}$ gap of a NIM/PIM Bragg grating can be exploited to enhance SHG from an interface by at least an order of magnitude for structures just a few tens of micrometers thick. Our findings thus suggest that standard centrosymmetric materials may be used to create a whole additional class of second-harmonic generation and nonlinear frequency conversion devices. One last note to point out is that in the kind of structures proposed here an angular tuning of the FF and SH on the proper resonances may be much easier to realize than in conventional photonic band gap structures because the location and the width of the zero-$\bar{n}$ gap are relatively insensitive to the angular incidence. Therefore one may think to align the SH on the proper resonance by angular tuning while the FF remains fixed on the band edge transmission resonance of the zero-$\bar{n}$ gap.

G.D'A. thanks the NRC for financial support.

[1] Y. R. Shen, *The Principles of Nonlinear Optics* (Wiley & Sons, New York, 1984).
[2] P. Guyot-Sionnest, W. Chen, and Y. R. Shen, Phys. Rev. B **33**, 8254 (1986).
[3] G. D'Aguanno *et al.*, Opt. Lett. **24**, 1663 (1999).
[4] (a) Y. Dumeige *et al.*, Appl. Phys. Lett. **78**, 3021 (2001); (b) P. P. Markowicz *et al.*, *ibid.* **87**, 051102 (2005).
[5] J. B. Pendry, Phys. Rev. Lett. **85**, 3966 (2000), and references therein.
[6] R. A. Shelby, D. R. Smith, and S. Schultz, Science **292**, 77 (2001).
[7] C. G. Parazzoli *et al.*, Phys. Rev. Lett. **90**, 107401 (2003).
[8] V. G. Veselago, Sov. Phys. Usp. **10**, 509 (1968).
[9] Jensen Li *et al.*, Phys. Rev. Lett. **90**, 083901 (2003).
[10] I. V. Shadrivov, A. A. Sukhorukov, and Y. S. Kivshar, Appl. Phys. Lett. **82**, 3820 (2003).
[11] Haitao Jiang *et al.*, Appl. Phys. Lett. **83**, 5386 (2003).
[12] R. S. Hedge and H. G. Winful, Opt. Lett. **30**, 1852 (2005).
[13] R. W. Ziolkowski, Opt. Express **11**, 662 (2003).
[14] G. D'Aguanno *et al.*, Phys. Rev. E **70**, 016612 (2004).
[15] N. Mattiucci *et al.*, Phys. Rev. E **72**, 066612 (2005).
[16] M. Scalora *et al.*, Phys. Rev. A **56**, 3166 (1997).
[17] V. Podolskiy, A. K. Sarychev, and V. M. Shalev, Opt. Express **11**, 735 (2003).
[18] S. Linden *et al.*, Science **306**, 1351 (2004).
[19] Shuang Zhang *et al.*, Phys. Rev. Lett. **94**, 037402 (2005).
[20] Shuang Zhang *et al.*, Phys. Rev. Lett. **95**, 137404 (2005).
[21] C. Enkrich *et al.*, Phys. Rev. Lett. **95**, 203901 (2005).
[22] F. Garwe *et al.*, Proc. SPIE **5955**, 59550T (2005).
[23] A. Ishikawa *et al.*, Phys. Rev. Lett. **95**, 237401 (2005).
[24] I. V. Shadrivov, A. A. Sukhorukov, and Y. S. Kivshar, Phys. Rev. Lett. **95**, 193903 (2005).
[25] W. Ziolkowski and E. Heyman, Phys. Rev. E **64**, 056625 (2001).
[26] R. W. Ziolkowski and A. D. Kipple, Phys. Rev. E **68**, 026615 (2003).
[27] R. W. Ziolkowski, Phys. Rev. E **70**, 046608 (2004).
[28] G. D'Aguanno *et al.*, Phys. Rev. Lett. **93**, 213902 (2004).
[29] G. D'Aguanno *et al.*, Opt. Lett. **30**, 1998 (2005).